

# Stability of droplets and channels on homogeneous and structured surfaces

P. Lenz<sup>a</sup> and R. Lipowsky<sup>b</sup>

Max-Planck-Institut für Kolloid- und Grenzflächenforschung, 14424 Potsdam, Germany

Received 4 August 1999

**Abstract.** Wetting of structured or imprinted surfaces which leads to a variety of different morphologies such as droplets, channels or thin films is studied theoretically using the general framework of surface or interface thermodynamics. The first variation of the interfacial free energy leads to the well-known Laplace equation and a generalized Young equation which involves spatially dependent interfacial tensions. Furthermore, we perform the second variation of the free energy for arbitrary surface patterns and arbitrary shape of the wetting morphology in order to derive a new and general stability criterion. The latter criterion is then applied to cylindrical segments or channels on homogeneous and structured surfaces.

**PACS.** 68.45.Gd Wetting – 68.10.Cr Surface energy (surface tension, interface tension, angle of contact, etc.) – 47.20.Dr Surface-tension-driven instability

## 1 Introduction

During the last years, several experimental methods have been developed by which a substrate can be laterally structured ([1–9]), *i.e.* endowed with a pattern of spatial regions (domains) with modified chemical and physical properties. A brief review of these methods can be found *e.g.* in references [10, 11]. If a liquid wets such a structured or imprinted surface, then the interface between the wetting layer and the substrate has a position-dependent free energy which reflects the underlying surface pattern. As a result, the shape of the wetting layer will be influenced by the 2-dimensional structure of the substrate. This interplay between the pattern of surface domains and the wetting layer morphology leads to new wetting phenomena such as non-spherical droplet shapes which can undergo shape instabilities [12] and morphological transitions between different wetting states [13].

Such morphological wetting transitions are a generic feature for wetting of structured surfaces. They are intimately related to the fact that droplets on surface domains can exhibit contact angles which do not fulfil the classical Young equation. To be more precise, depending on its volume, a droplet belongs to one of three droplet regimes, in the sequel denoted as droplet regimes (I), (II) and (III). If a hydrophobic substrate with a single hydrophilic domain is considered, then regime (I) corresponds to a contact area between droplet and surface which is smaller than the surface domain. In regime (II) the hydrophilic region is completely covered and in regime (III) the droplet spreads

onto the hydrophobic substrate. Whereas in regime (I) and (III), the Young equation is fulfilled, the contact angle in regime (II) is determined by the volume<sup>1</sup> of the droplet only, see reference [13]. One should note that the droplets belonging to droplet regimes (I)–(III) are in (mechanical) equilibrium. However, in experiments situations can be encountered where the (interfacial) forces acting on the droplet are not balanced out leading thus to various additional dynamical droplet regimes, see *e.g.* references [15, 16].

Since in regime (II) the hydrophilic domains are completely covered, the morphology of the wetting layer can be influenced in a controlled way by prescribing the contact area with appropriately chosen domain geometries. As an example, liquid channels were realized in reference [12] by prescribing rectangular contact areas. Such morphologies of the wetting layer are unstable on homogeneous substrates where they decay into a chain of (spherical) droplets. On structured surfaces they are stabilized against this classical Rayleigh-Plateau instability, but exhibit a new kind of instability leading to a channel with a single bulge.

The aim of the present article is to deepen the formal understanding of the difference between the instability of wetting layer morphologies on structured and on homogeneous substrates. To reach this goal, a general classification of the stationary states and a general investigation of their stability is necessary. This will be done here by

---

<sup>1</sup> Our approach can be extended to the grand-canonical ensemble where morphological transitions can occur for wetting layers on scales comparable with the range of the microscopic forces. One example is provided in reference [14].

---

<sup>a</sup> e-mail: lenz@cmtql.harvard.edu

<sup>b</sup> e-mail: lipowsky@mpikg-golm.mpg.de

deriving a general stability criterion valid for stationary morphologies of the wetting layer on homogeneous and structured substrates.

The experimentally observable droplet shapes are given by the minima of the free energy  $F$  of the system. These correspond to wetting morphologies which are solutions of the Laplace equation, *i.e.* morphologies with a liquid-vapor interface which is a surface of constant mean curvature and which fulfills the geometrical boundary conditions<sup>2</sup>. However, not all solutions of the Laplace equation correspond to minima of  $F$ . In general, they only correspond to stationary states of the free energy. They are not necessarily stable, but could correspond to a maximum or a saddle point of the free energy. Thus, in order to determine the stable solutions one has to investigate the local behavior of the free energy. By performing a linear stability analysis of the stationary states the solutions corresponding to the minima can be classified. In this method, the state under investigation is transformed to a neighboring state of the configuration space by a small perturbation. Since the original state is stationary, the free energy changes only in second order of this perturbation. As in the case of regular functions, the eigenvalues of this second variation  $\delta^{(2)}F$  reflect the local behavior of  $F$  at the stationary points. The stationary state is a minimum if all eigenvalues are positive, it corresponds to a maximum if all are negative.

If the eigenvalues depend, in general, on external parameters, a change of these parameters can lead to a change of the local behavior of the functional at the stationary state. In the situation considered here, the eigenvalues depend on  $V$ , the volume of the droplet. If for a certain volume range  $V < V^{\max}$  all eigenvalues of a morphology ( $A$ ) are positive and if for  $V > V^{\max}$  at least one eigenvalue is negative, then the state ( $A$ ) becomes unstable at  $V = V^{\max}$ . For  $V > V^{\max}$  there must be a different minimum ( $B$ ) in the configuration space and one encounters a physical situation where a morphological transition between ( $A$ ) and ( $B$ ) takes place<sup>3</sup>. For a first order transition between ( $A$ ) and ( $B$ ) the spinodal transition, *i.e.* the transition where no activation barriers has to be overcome, takes place at  $V^{\max}$ . Then, ( $A$ ) is already only metastable in a volume range  $V^* < V < V^{\max}$ . If the transition is second order, then it takes place at the critical volume  $V^{\max}$ . One should be aware that with the help of the stability analysis neither the state ( $B$ ) nor the order of the transition can be determined. Analytical methods which go beyond this linear approximation in the context of wetting on structured surfaces are described elsewhere [13, 19].

<sup>2</sup> Here, the question under which conditions such solutions exist shall not be considered. Corresponding investigations can be found in the mathematical literature, see *e.g.* references [17, 18].

<sup>3</sup> In the system considered here, fluctuations are very weak at room temperature  $T$ . Thus, even though the system is finite and  $T > 0$ , this transition leads to an experimentally observable sharp change in the morphology.

One possibility to realize this program is to chose suitable coordinates for a given geometry of the surface domains. For example, the droplets could be parameterized by cylindrical coordinates or by the Monge representation. The free energy is then a functional of the radius vector  $r(\varphi, z)$  or of the height function  $h(x, y)$ . The displacement of the configuration is given by a displacement of  $r$  and  $h$ , respectively. The second variation  $\delta^{(2)}F$  can be calculated by expanding the functional in this perturbation. However, one should be aware that this is a variational problem with constraints. Not all displacements are allowed since the contact line of the perturbed configuration has to stay on the substrate. The corresponding additional constraints have to be taken into account in order to determine the appropriate eigenmodes [20, 21]. Although it is often more convenient to calculate in given coordinates, the main disadvantage of such a procedure is that one obtains results which depend on the chosen parameterization.

For that reason a different approach shall be pursued here. Formally, the liquid-vapor interface bounding the wetting layer in three dimensions represents a two-dimensional surface which can be parameterized by local coordinates. In this formulation, the free energy has a functional dependence on the geometry of the interface. With the help of the local calculus of differential geometry it is possible to expand the change in the free energy caused by a general displacement in terms of the small parameters of this displacement. In particular, it is then possible to calculate the second variation of the free energy in a coordinate independent fashion. The corresponding calculation is somewhat tedious but the final result holds both for homogeneous and for structured substrates with arbitrary surface domain geometries. Furthermore, if the general stability criterion is evaluated in special systems the most convenient coordinates for the particular geometry can be chosen.

Similar coordinate independent formulations have been used previously for related problems. For example, this calculus can also be used to derive the shape equation of minimal surfaces [22], to investigate the stability of fluid [23] or polymerized vesicles [24]. Compared to these previous studies the main technical difficulty, which arises from the application of these methods to wetting morphologies, is the treatment of the boundary conditions originating from the presence of the wall.

This paper is organized as follows. First, the theoretical framework necessary to describe the wetting morphologies is introduced in Section 2. Then, in Section 3 the coordinate independent parameterization of the droplet shapes is introduced and the functional dependence of the free energy on the geometry of the system is discussed. Afterwards, the change of metric and the change of the various contributions to the free energy caused by the perturbation of the stationary state is calculated. The first- and second-order contributions of this general expansion yield the conditions for the stationary states and the general stability criterion, respectively. Finally, in Section 5 this general stability criterion is applied to special geometries.

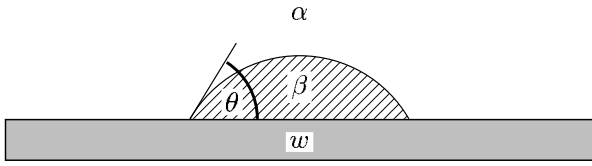


**Fig. 1.** Partial wetting of a substrate  $w$  by a droplet of phase  $(\beta)$  in the presence of a third phase  $(\alpha)$ . The shape of the droplet is characterized by a contact angle  $\theta$ , which is here measured inside the droplet.

## 2 Free energy of droplet

As mentioned in the introduction, a physical situation shall be considered where two fluid phases are in contact with a wall or a solid substrate. The theoretical description given below holds both for a liquid vapor system and a binary mixture of liquids which wet either a homogeneous or a structured substrate.

To proceed, denote the vapor and the liquid phase by  $(\alpha)$  and  $(\beta)$ , and the hydrophilic and hydrophobic surface regions by  $(\gamma)$  and  $(\delta)$ , respectively, see also Figure 1. The interfacial region between phase  $(i)$  and phase  $(j)$  has surface area  $A_{ij}$  and interfacial tension  $\Sigma_{ij}$ .

In the following, we will concentrate on domains and corresponding droplets in the micrometer-range. Then, the free energy of a wetting layer consists of the contributions arising from the interfacial free energy of the  $(\alpha\beta)$  interface, from the free energy of wetting the contact area and from the volume. For convenience, all free energies are given in units of the interfacial tension  $\Sigma_{\alpha\beta}$ . The equilibrium state of the wetting layer with prescribed volume  $V$  then corresponds to the global minimum of the free energy functional as given by [13,10]

$$F = F_{\alpha\beta} + F_{\beta w} + \frac{\Delta P}{\Sigma_{\alpha\beta}} V$$

$$\equiv \int dA_{\alpha\beta} - \int dA_{\beta w} \cos \theta_{\beta w} + \frac{\Delta P}{\Sigma_{\alpha\beta}} \int dV, \quad (1)$$

with  $w = \gamma$  or  $w = \delta$ . If larger length scales are considered, gravity has to be taken into account (see *e.g.* Refs. [25–28]), while for smaller scales corrections arising from line tensions (see *e.g.* Refs. [29,30]) and intermolecular interactions will become important [31,32].

Here,  $dA_{\alpha\beta} \equiv dA$  denotes the area element of the  $(\alpha\beta)$  interface,  $dA_{\beta w}$  the contact area element and  $dV$  the volume element. If structured substrates are considered, the interfacial tensions have a position dependency which reflects the underlying surface pattern [13]. Then, the contact angle  $\theta_{\beta w}$  is *defined* by

$$\cos \theta_{\beta w} \equiv \frac{\Sigma_{\alpha w} - \Sigma_{\beta w}}{\Sigma_{\alpha\beta}}. \quad (2)$$

Nevertheless, equation (1) holds both for wetting layer morphologies on homogeneous and for morphologies on

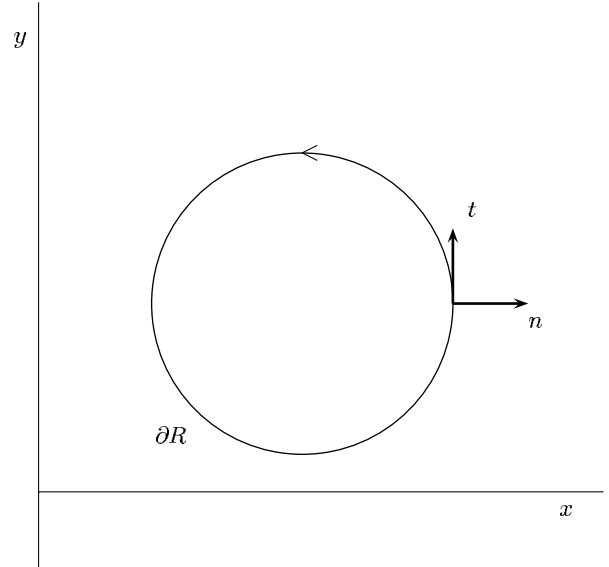


**Fig. 2.** Definition of normal vector  $n(s)$  and tangential vector  $t(s)$  of the contact line  $\partial R$ . All integrals are performed in a counterclockwise fashion (when viewed from the half space with positive  $z$ ).

structured surfaces. For structured surfaces  $\theta_{\beta w} = \theta_{\beta w}(x)$ , *i.e.* the interfacial tensions depend on the position  $x$  on the surface. If  $\theta(s)$  denotes the contact angle at the position  $s$  of the contact line  $\partial R$ , then  $\theta(s) = \theta_{\beta\gamma} \equiv \theta_\gamma$  if  $\partial R(s)$  lies on  $(\gamma)$  and  $\theta(s) = \theta_{\beta\delta} \equiv \theta_\delta$  if  $\partial R(s)$  lies on  $(\delta)$ , see Figure 2. On the other hand, for homogeneous substrates  $\theta(s) = \theta_{\beta w}$  for all positions  $s$  on the tripelline.

Finally,  $\Delta P \equiv P_\alpha - P_\beta$  denotes the pressure difference between outside and inside the droplet. Due to the curvature of the  $(\alpha\beta)$ -interface the pressure is increased inside the droplet, *i.e.*  $P_\beta > P_\alpha$ . The physical meaning of this parameter depends on the ensemble one is considering. Here, in an ensemble of constant volume,  $\Delta P$  is a Lagrange multiplier which guarantees that the constraint on the volume is fulfilled.

## 3 Parameterization of droplet shape

As explained in the introduction, the aim of this study is to investigate the stability of droplets which are stationary states of the free energy. To perform this analysis in a coordinate independent fashion, it is useful to parameterize the  $(\alpha\beta)$ -interface by its surface vector  $R: \Omega \rightarrow \mathbb{R}^3$ . Here,  $(s^1, s^2) \in \Omega$  are local coordinates. Then, the free energy (1) becomes a functional of the vector  $R(s^1, s^2)$ . To be more precise, it depends on the two fundamental forms determined by  $R$ , which characterize the geometrical properties of this surface and, thus, of the droplet shape. In order to determine the stability of a stationary state  $R$ , one has to investigate the local behavior of  $F[R]$  by considering a surface  $R' = R + \delta R$  which lies in the infinitesimal neighborhood of  $R$ . Then, the free energy  $F[R']$  of  $R'$  has to be compared with that of  $R$ . As shown

in the following, it is possible to express the second variation  $\delta^{(2)}F$  in terms of the second-order perturbation  $\delta^{(2)}R$  by using the local calculus of differential geometry. Hence, it is possible to calculate the second variation of the free energy in a coordinate independent fashion.

### 3.1 Differential geometry of shape

Here, we collect various formulas from differential geometry which refer to the droplet shape, *i.e.* formulas which relate  $R$  and its derivatives with fundamental geometrical quantities.

The surface area and the volume depend on the metric, given by the first fundamental form

$$g_{ij} \equiv R_i \cdot R_j, \quad (3)$$

with the covariant vector  $R_j \equiv R_{,j} \equiv \partial_{s^j} R \equiv \partial R / \partial s^j$ . The contravariant components are given by  $R^k = g^{ki} R_i$ , with  $g^{ij} g_{jk} = \delta_k^i$ , see Appendix A. Here and below, it is understood that repeated indices are summed over. The position of the index thus determines the behavior under transformations. If a coordinate change  $s \rightarrow \bar{s}$  is considered, then the transformation of covariant vectors is given by the Jacobian of the coordinate change, whereas the contravariant vectors transform *via* the inverse of the Jacobian as given by

$$R_i(\bar{s}) = \frac{\partial s^k}{\partial \bar{s}^i} R_k(s) \quad \text{and} \quad R^i(\bar{s}) = \frac{\partial \bar{s}^i}{\partial s^k} R^k(s). \quad (4)$$

The area element depends on the first fundamental form  $dA = \sqrt{g} ds^1 ds^2$  with

$$g \equiv \det(g_{ij}) = \frac{1}{2} \varepsilon^{ij} \varepsilon^{kl} g_{ik} g_{jl}. \quad (5)$$

Here,  $\varepsilon^{ij} = \varepsilon_{ij}$  denotes the two-dimensional Levi-Civita symbol, see Appendix A.

The second fundamental form is defined as

$$h_{ij} \equiv R_{ij} \cdot N = -R_i \cdot N_j, \quad (6)$$

where  $N(s^1, s^2) \equiv R_1(s^1, s^2) \times R_2(s^1, s^2) / \sqrt{g}$  denotes the (local) normal vector to the surface. The curvature of the surface is determined by  $h_{ij}$ . The mean curvature  $H$  and the Gaussian curvature  $K$  are given by

$$2H = -h_i^i \quad \text{and} \quad K = \det(h_j^i) = \frac{h}{g} \equiv \frac{\det(h_{ij})}{\det(g_{ij})}. \quad (7)$$

The variation of the droplet shape as discussed below will lead to contributions depending on  $R_{ij}$  and  $N_i$ . The second derivatives  $R_{ij}$  can be expressed as

$$R_{ij} = \Gamma_{ij}^k R_k + h_{ij} N, \quad (8)$$

since  $R_i$  and  $N$  form a local basis.

The coefficients  $\Gamma_{ij}^k$  are the Christoffel symbols of the second kind. They are related to the Christoffel symbols of the first kind *via*

$$\Gamma_{ikj} = g_{kl} \Gamma_{ij}^l \quad \text{with} \quad \Gamma_{ikj} \equiv \frac{1}{2} (\partial_i g_{kj} + \partial_j g_{ik} - \partial_k g_{ij}), \quad (9)$$

see reference [22]. In this convention, the Christoffel symbols of the first kind  $\Gamma_{ikj}$  are symmetric in the first and last index

$$\Gamma_{ikj} = \Gamma_{jki}. \quad (10)$$

Furthermore, they are related to the first fundamental form *via*

$$\Gamma_{jk}^j = \frac{1}{\sqrt{g}} \left( \frac{\partial}{\partial s^k} \sqrt{g} \right) \equiv \frac{(\sqrt{g})_{,k}}{\sqrt{g}}, \quad (11)$$

where the notation “ $k$ ” denotes a derivative with respect to  $s^k$ .

Finally, the Weingarten equations (see *e.g.* [22]) as given by

$$N_i = -h_i^k R_k, \quad (12)$$

express the change of the normal vector in terms of the two tangent vectors. From the last equation and the Hamilton-Cayley theorem (see *e.g.* [33]) one obtains the useful relation

$$h_i^n h_{nl} = -2H h_{il} - K g_{il}. \quad (13)$$

Likewise, one has  $h_{il} h^{li} = 4H^2 - 2K$ .

### 3.2 Displacement of shape

In order to determine the stationary states of the free energy  $F$  and to investigate their stability, it is necessary to transform a given configuration  $R$  into a neighboring configuration  $R'$ , see Figure 3. At every point  $R = R(s^1, s^2)$ , a local basis is given by  $R_1$ ,  $R_2$  and  $N$ . Hence, the displacement  $R' - R$  is a linear combination of these basis vectors and one has

$$R' = R + \eta^i R_i + \psi N, \quad (14)$$

with local coefficients  $\psi = \psi(s^1, s^2)$  and  $\eta^i = \eta^i(s^1, s^2)$ ,  $i = 1, 2$ . Note, that we use the same intrinsic coordinates for both  $R$  and  $R'$ .

Thus, a general displacement consists of a normal and a tangential component. For free droplets, it is sufficient to consider only normal displacements ( $\eta^i \equiv 0$ ) since the tangential displacement only reparameterizes the normal one. However, in the system considered here, the presence of the substrate surface leads to additional boundary conditions, since the contact line of  $R'$  has to lie on this surface. This requirement can not be fulfilled by considering only normal displacements (as can be seen *e.g.* by disturbing a cylindrical segment with contact angle  $0 < \theta < \pi/2$ ) and

$$\begin{aligned}
\delta g/g &= \frac{2}{\sqrt{g}} \left( \eta^i \sqrt{g} \right)_{,i} + 4H\psi + \psi^2(4H^2 + 2K) + \psi^i \psi_i + \det(\eta_{,i}^j + \eta_i^{,j}) \\
&+ \eta_{,i}^k \eta_k^i - 2\psi \eta_i^l h_l^i + 2\psi^j \eta^l h_{jl} - 2H\eta^k \eta^l h_{kl} - K\eta^l \eta_l - 2\psi \varepsilon^{ik} \varepsilon_{jl} h_k^l \left( \eta_{,i}^j + \eta_i^{,j} \right) \\
&+ 2\eta_l^j \Gamma_{jk}^l \eta^k + \eta^m \eta^n \Gamma_{im}^k \Gamma_{jn}^l g^{kl} - 2\psi h_k^i \eta^m \Gamma_{im}^k + \det(\lambda_i^j) + \varepsilon^{ik} \varepsilon_{jl} \lambda_k^l \left( \eta_{,i}^j + \eta_i^{,j} - 2\psi h_i^j \right) + \mathcal{O}(\psi^3, \eta^3). \quad (24)
\end{aligned}$$

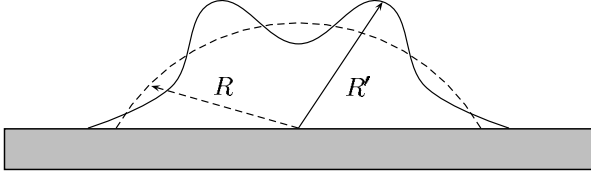


**Fig. 3.** Perturbation of a stationary configuration parameterized by the surface vector  $R$  into a neighboring one parameterized by  $R'$ .

one has to introduce tangential displacements. Far from the contact line, the tangential displacements  $\eta^i$  still lead only to a reparameterization of  $\psi$ . It is therefore sufficient to consider displacements  $\eta^i$  which vanish at a certain distance from the contact line.

As the following investigation shows, it is possible with the help of the local calculus of differential geometry to express  $F[R']$  in terms of  $R$ ,  $\psi$  and  $\eta^i$ . For a linear stability analysis it is sufficient to consider only small displacements. Then, the second variation of the free energy is given by an expansion up to second order in  $\psi$  and  $\eta^i$ .

Before calculating the difference  $F[R'] - F[R]$  one has to determine the *change of metric* caused by the displacement. The new tangent vectors are given by

$$R'_i = R_i + \xi_i^k R_k + \nu_i N, \quad (15)$$

with

$$\xi_i^k = \eta_{,i}^k + \eta^j \Gamma_{ij}^k - \psi h_i^k \quad \text{and} \quad \nu_i = \psi_i + \eta^j h_{ij}, \quad (16)$$

where equations (8, 12) have been used. Here,  $\eta_{,i}^k = \partial \eta^k / \partial s^i$ . This notation has been introduced in order to distinguish between  $\eta_{,i}^k$  and  $\eta_k^i$ . This is for later convenience. In order to have more freedom in the choice of  $\eta^i$  it is useful not to assume that  $\eta = (\eta^1, \eta^2)$  is a differential, *i.e.* it shall not be assumed that a function  $f$  exists with  $f_i = f_{,i} = \eta_i = g_{ij} \eta^j$ . Furthermore, one should note that generally  $\xi_{jk} \neq \xi_{kj}$ .

The first fundamental form then changes as

$$\begin{aligned}
\delta g_{ij} &\equiv g'_{ij} - g_{ij} \\
&= R'_i \cdot R'_j - R_i \cdot R_j \\
&= \xi_j^k g_{ik} + \xi_i^k g_{kj} + \xi_i^k \xi_j^l g_{kl} + \nu_i \nu_j. \quad (17)
\end{aligned}$$

By using equation (A.7) one obtains

$$\begin{aligned}
\delta g &\equiv g' - g \\
&= g g^{ij} \delta g_{ij} + \frac{1}{2} \varepsilon^{ik} \varepsilon^{jl} \delta g_{kl} \delta g_{ij} \\
&\equiv \delta g_1 + \det(A_{ij}) + \mathcal{O}(\eta^3, \psi^3), \quad (18)
\end{aligned}$$

with

$$A_{ij} \equiv \eta_{i,j} + \eta_{j,i} + \eta^l (\Gamma_{lij} + \Gamma_{lji}) - 2\psi h_{ij} \quad (19)$$

$$\delta g_1 = g (2\xi_i^i + \xi_i^k \xi_j^l g^{kl} + \nu_i \nu^i). \quad (20)$$

By using the identities (A.9, A.10, 13) one obtains

$$\begin{aligned}
\det(A_{ij})/g &= \det(\eta_{,i}^j + \eta_i^{,j}) + 4K\psi^2 + \det(\lambda_i^j) \\
&+ \varepsilon^{ik} \varepsilon_{jl} \left[ \lambda_k^l \left( \eta_{,i}^j + \eta_i^{,j} - 2\psi h_i^j \right) \right. \\
&\quad \left. - 2\psi h_k^l (\eta_{,i}^j + \eta_i^{,j}) \right], \quad (21)
\end{aligned}$$

with

$$\begin{aligned}
\lambda_{kl} &\equiv \eta^m (\Gamma_{mkl} + \Gamma_{mlk}), \\
\lambda_k^l &\equiv \lambda_{ks} g^{sl} = \eta^m (\Gamma_{mks} g^{sl} + \Gamma_{mk}^l). \quad (22)
\end{aligned}$$

The term  $\delta g_1$  can be treated in a similar way. In particular, one obtains from equation (11) that

$$\xi_j^j = \frac{1}{\sqrt{g}} \left( \eta^i \sqrt{g} \right)_{,i} + 2H\psi. \quad (23)$$

Finally, by collecting all contributions, one ends up with

*see equation (24) above.*

## 4 Variation of droplet free energy

Now, the change in the free energy caused by the displacement  $R \rightarrow R'$  can be calculated. The contributions which have to be taken into account are: (i) change of the  $(\alpha\beta)$  interfacial area; (ii) change of the contact area; and (iii) change of the volume. Correspondingly, one has to calculate the contributions (i)  $\delta F_{\alpha\beta}$ ; (ii)  $\delta F_{\beta w}$ ; and (iii)  $\delta V$ .

The difference in the free energy  $F[R'] - F[R]$  will be expanded in  $\psi$  and  $\eta^i$ . The expansion up to first order gives the first variation of the free energy. By requiring that this variation vanishes, one obtains the Laplace equation and a generalized Young equation. The expansion up to second order in the coefficients  $\psi$  and  $\eta^i$  then determines the second variation of the free energy, which leads to a general stability criterion for the stationary states.

$$\begin{aligned}
a^{(2)} \equiv & K\psi^2 + \frac{1}{2} \left( \psi^i \psi_i + \eta_i^k \eta_k^l - \eta_i^i \eta_j^j \right) - 2H\psi\eta_i^i + \frac{1}{2} \det(\eta_i^j + \eta_i^j) - \psi \left( \eta_i^l h_i^l + \varepsilon^{ik} \varepsilon_{jl} h_k^l \left( \eta_i^j + \eta_i^j \right) \right) \\
& + \psi^j \eta^l h_{jl} - H\eta^k \eta^l h_{kl} - \frac{1}{2} K \eta^l \eta_l + \frac{1}{2} \left( \eta^m \eta^n \Gamma_{im}^k \Gamma_{jn}^l g^{ij} g_{kl} - \eta^m \eta^n \Gamma_{km}^k \Gamma_{ln}^l + \det(\lambda_i^j) \right) + \eta_i^j \Gamma_{jk}^l \eta^k \\
& - \psi h_k^i \eta^m \Gamma_{im}^k - \Gamma_{mj}^m (\eta_i^i \eta^j + 2H\psi\eta^j) + \frac{1}{2} \varepsilon^{ik} \varepsilon_{jl} \lambda_k^l \left( \eta_i^j + \eta_i^j - 2\psi h_i^j \right). \tag{27}
\end{aligned}$$

#### 4.1 Area change of the fluid-vapor interface

Here, the change in free energy associated with the area-change of the  $(\alpha\beta)$ -interface will be calculated. In the following, the first-order contributions shall be partitioned into two parts denoted by  $\delta^{(1)}F_{\alpha\beta}$  and  $\delta^{(1)}F_{\alpha\beta}^*$ . Here,  $\delta^{(1)}F_{\alpha\beta}^*$  is given by the terms depending on  $\eta^i$ , whereas  $\delta^{(1)}F_{\alpha\beta}$  depends on  $\psi$  only. Hence,  $\delta^{(1)}F_{\alpha\beta}^*$  will contribute to the transversality condition of the variational problem, whereas  $\delta^{(1)}F_{\alpha\beta}$  will determine the Euler-Lagrange equation. The second-order contributions shall be denoted by  $\delta^{(2)}F_{\alpha\beta}$ . Therefore,

$$\begin{aligned}
\delta F_{\alpha\beta} &= \int_{\Omega} ds^1 ds^2 \left( \sqrt{g + \delta g} - \sqrt{g} \right) \\
&= \delta^{(1)}F_{\alpha\beta} + \delta^{(1)}F_{\alpha\beta}^* + \delta^{(2)}F_{\alpha\beta} + \mathcal{O}(\eta^3, \psi^3), \tag{25}
\end{aligned}$$

with

$$\begin{aligned}
\delta^{(1)}F_{\alpha\beta} &\equiv \int_{\Omega} dA 2H\psi, \\
\delta^{(1)}F_{\alpha\beta}^* &\equiv \int_{\Omega} dA \frac{1}{\sqrt{g}} \left( \eta^i \sqrt{g} \right)_{,i}, \\
\delta^{(2)}F_{\alpha\beta} &\equiv \int_{\Omega} dA a^{(2)}. \tag{26}
\end{aligned}$$

Here, all integrals extend over the domain  $\Omega$  of intrinsic coordinates  $(s^1, s^2)$ .

The second order contribution is given by

*see equation (27) above.*

By using the Gauss (or Green) theorem in two dimensions one obtains

$$\delta^{(1)}F_{\alpha\beta}^* = \int_{\partial\Omega} \sqrt{g} (\eta^1 ds^2 - \eta^2 ds^1), \tag{28}$$

where the line integral is performed in a counterclockwise fashion<sup>4</sup>, see Figure 2. This can be rewritten using [22]

$$\sqrt{g} (\eta^1 ds^2 - \eta^2 ds^1) = (R' - R) \cdot (dR \times N), \tag{29}$$

<sup>4</sup> Sometimes, it is more convenient to choose a clockwise orientation of  $\partial R$ , since then  $(t, n, e_z)$  is a right-handed coordinate system. If such a parameterization is chosen here, equation (28), correspondingly equation (31) and the first term of equation (32) change sign, therefore also equation (42). However, the second term in equation (32) and correspondingly in equation (46) do not change their sign.

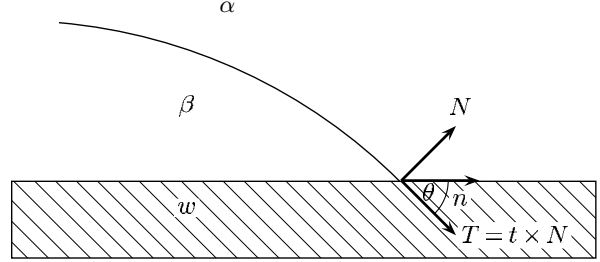


**Fig. 4.** Definition of normal vector  $N(s)$ , the tangential vector  $T(s)$  and the contact angle  $\theta$  of the surface  $R$  at the contact line.

with  $dR = R_1 ds^1 + R_2 ds^2$ . If  $\omega(s)$  is a representation of  $\partial\Omega$  in terms of the arclength  $s$  of the contact line  $\partial R \equiv R|_{\partial\Omega}$  (that is the restriction of  $R(s^1, s^2)$  on the border of  $\Omega$ ), then  $dR(\omega(s)) = t(s)ds$  holds, with the tangent vector  $t(s)$  of the boundary. The tangent vector  $T(s)$  of the droplet is then given by

$$T(s) \equiv t(s) \times N(\omega(s)), \tag{30}$$

as illustrated in Figure 4. Thus, one arrives at

$$\begin{aligned}
\delta^{(1)}F_{\alpha\beta}^* &= \int_{\partial\Omega} (R' - R) \cdot (dR \times N) \\
&= \int_{\partial R} ds (R'(s) - R(s)) \cdot T(s). \tag{31}
\end{aligned}$$

#### 4.2 Change of contact area with solid wall

Next, the change of the free energy arising from the change of the wetted area will be calculated. Again, this contribution will be split up into the first-order contribution  $\delta^{(1)}F_{\beta w}$  and the second-order contribution  $\delta^{(2)}F_{\beta w}$ .

In this study, only planar substrates shall be considered. It is therefore sufficient to consider only normal displacements of the contact line for which  $R'(s) - R(s)$  is parallel to  $n(s)$  at the tripeline, with  $n(s)$  denoting the (outward) normal vector of the contact line, see Figure 4. The change of contact area is then given by a sum over rectangles with area  $|R' - R|ds$  and triangles with area  $(1/2)|R' - R||n \times n_s|ds$ . By using the Frenet formulas

(see *e.g.* Ref. [34]) one obtains

$$\begin{aligned} \delta F_{\beta w} &= \delta^{(1)} F_{\beta w} + \delta^{(2)} F_{\beta w} + \mathcal{O}(\eta^3, \psi^3) \\ &\equiv - \int_{\partial R} ds \cos \theta_{\beta w} (\psi N + \eta^i R_i) \cdot n(s) \\ &\quad - \frac{1}{2} \int_{\partial R} ds \cos \theta_{\beta w} (\psi^2 + \eta^i \eta_i) C(s) + \mathcal{O}(\eta^3, \psi^3). \end{aligned} \quad (32)$$

Here,  $C(s)$  denotes the curvature of the contact line. The sign of  $C(s)$  is chosen in such a way that the curvature of a circle of radius  $r$  is positive and given by  $C = 1/r$ . The restriction  $R'(s) - R(s)$  parallel to  $n(s)$  implies that the tangential displacements have to be parallel to the tangent vector  $T(s)$ , *i.e.*

$$\eta^i R_i = \xi T \text{ on the contact line } \partial R, \quad (33)$$

with some function  $\xi$ . Thus  $\psi N + \xi T$  is parallel to  $n$  everywhere at the tripelline and the scalar product of the substrate normal and  $\psi N + \xi T$  must vanish, which implies

$$\psi(s) \cos \theta(s) - \xi(s) \sin \theta(s) = 0, \quad (34)$$

since the local contact angle  $\theta(s)$  is the angle between  $n(s)$  and  $T(s)$ . One may set

$$\xi(s) \equiv \tau(s) \cos \theta(s) \quad \text{and} \quad \psi(s) \equiv \tau(s) \sin \theta(s), \quad (35)$$

with an arbitrary function  $\tau(s)$ .

### 4.3 Change of volume

Finally, the change of the volume  $\delta V$  caused by the displacement  $R' - R$  has to be determined. It can be written as a sum of properly chosen polyhedra

$$\delta V = \int ds^1 ds^2 \Delta V(s^1, s^2). \quad (36)$$

Here,  $V_P \equiv ds^1 ds^2 \Delta V(s^1, s^2)$  is the volume of the polyhedron with the upper and lower face given by the parallelograms spanned by the vectors

$$(R_1(s^1, s^2) ds^1, R_2(s^1, s^2) ds^2)$$

and

$$(R'_1(s^1, s^2) ds^1, R'_2(s^1, s^2) ds^2).$$

These two parallelograms are connected by the vector  $\psi N + \eta^i R_i$ . With the help of the Gauss theorem the volume  $V_P$  can be calculated. By introducing Cartesian coordinates with the  $z$ -axis parallel to  $\psi N + \eta^i R_i$  and origin at  $(\psi N + \eta^i R_i)/2$  one obtains

$$V_P = \int_{V_P} dV = \int_{V_P} dV \operatorname{div}(z e_z) = \int_{\partial V_P} dA \cdot e_z z, \quad (37)$$

where  $\partial V_P$  denotes the surface of the polyhedron.

As shown in Appendix B, the side faces contribute only in higher order  $\mathcal{O}(\psi^3, \eta^3)$ . Then, the only relevant contribution is that of the upper and lower face. Here,  $z e_z \cdot dA = (1/2)(\psi N + \eta^i R_i) \cdot dA + \mathcal{O}((ds^1)^2 ds^2, (ds^2)^2 ds^1)$  holds, since  $dA$  is already of the order  $ds^1 ds^2$ . Therefore,

$$\begin{aligned} \Delta V &= \frac{1}{2} (\psi N + \eta^i R_i) \cdot (R_1 \times R_2 + R'_1 \times R'_2) + \mathcal{O}(\psi^3, \eta^3) \\ &= \sqrt{g} \left( \psi + H \psi^2 + \frac{1}{2} \eta_{,i}^i \psi + \frac{1}{2} \eta^j \Gamma_{ij}^i \psi - \frac{1}{2} \eta^i \psi_i - \frac{1}{2} \eta^i \eta^j h_{ij} \right) \\ &\quad + \mathcal{O}(\psi^3, \eta^3). \end{aligned} \quad (38)$$

Thus, one ends up with the first and second order contributions

$$\delta^{(1)} V \equiv \int dA \psi \quad (39)$$

$$\begin{aligned} \delta^{(2)} V &\equiv \int dA v^{(2)} \\ &\equiv \int dA \left( H \psi^2 + \frac{1}{2} \eta_{,i}^i \psi + \frac{1}{2} \eta^j \Gamma_{ij}^i \psi \right. \\ &\quad \left. - \frac{1}{2} \eta^i \psi_i - \frac{1}{2} \eta^i \eta^j h_{ij} \right). \end{aligned} \quad (40)$$

### 4.4 First variation of free energy

The contributions arising from Sections 4.1–4.3 can be combined to

$$\begin{aligned} \delta F &= \delta^{(1)} F + \delta^{(2)} F + \mathcal{O}(\eta^3, \psi^3) \\ &\equiv \delta^{(1)} F_{1d} + \delta^{(1)} F_{2d} + \delta^{(2)} F + \mathcal{O}(\eta^3, \psi^3). \end{aligned} \quad (41)$$

The first-order contributions can be split up into a term  $\delta^{(1)} F_{1d}$  depending on  $\eta^i$  and into a term  $\delta^{(1)} F_{2d}$  independent of  $\eta^i$ . Then, the contributions  $\delta^{(1)} F_{\beta w}$  and  $\delta^{(1)} F_{\alpha\beta}^*$  determine  $\delta^{(1)} F_{1d}$

$$\begin{aligned} \delta^{(1)} F_{1d} &\equiv \delta^{(1)} F_{\beta w} + \delta^{(1)} F_{\alpha\beta}^* \\ &= \int_{\partial R} ds \tau(s) (\cos \theta(s) - \cos \theta_{\beta w}). \end{aligned} \quad (42)$$

The contribution independent of the subsidiary condition is given by

$$\delta^{(1)} F_{2d} = \delta^{(1)} F_{\alpha\beta} + \frac{\Delta P}{\Sigma_{\alpha\beta}} \delta^{(1)} V. \quad (43)$$

The terms  $\delta^{(1)} F_{1d}$  and  $\delta^{(1)} F_{2d}$  are independent. Hence, a stationary state has to fulfill  $\delta^{(1)} F_{1d} = 0$  and  $\delta^{(1)} F_{2d} = 0$  separately. These conditions are equivalent to the Laplace equation

$$\frac{\Delta P}{\Sigma_{\alpha\beta}} = -2H, \quad (44)$$

and a generalized Young equation

$$\begin{aligned} \cos \theta(p) &= \cos \theta_{\beta w}(p) \\ &\text{for all } p \in \partial R \text{ on the contact line.} \end{aligned} \quad (45)$$

#### 4.5 Second variation of free energy

In second order one obtains

$$\begin{aligned} \delta^{(2)}F &= \delta^{(2)}F_{\alpha\beta} + \frac{\Delta P}{\Sigma_{\alpha\beta}} \delta^{(2)}V + \delta^{(2)}F_{\beta w} \\ &= \int dA \left( a^{(2)} - 2Hv^{(2)} \right) \\ &\quad - \frac{1}{2} \int_{\partial R} ds \cos \theta_{\beta w} (\psi^2 + \eta^i \eta_i) C(s). \end{aligned} \quad (46)$$

This equation together with equations (27, 40) is the main result of this study. It is the desired coordinate independent stability criterion which is valid for arbitrary droplet morphologies on arbitrary domains.

### 5 Applications

Now, this general stability criterion can be applied to special geometries. The following investigation concentrate mainly on stripe domains. However, some results can be generalized to arbitrary domain geometries.

Generally, droplets on stripe domains are given by cylindrical segments with contact angle  $\theta = \theta(s)$  and radius  $R_{\text{cy}}$ . Then,

$$R = (R_{\text{cy}} \cos(\varphi + \pi/2 - \theta), R_{\text{cy}} \sin(\varphi + \pi/2 - \theta), z),$$

with  $\varphi \in [0, 2\theta]$ . By setting  $s^1 \equiv \varphi$  and  $s^2 \equiv z$  the non-vanishing elements of the first and second fundamental form are given by

$$g_{11} = R_{\text{cy}}^2, \quad g_{22} = 1, \quad h_{11} = -R_{\text{cy}}. \quad (47)$$

Hence,  $\sqrt{g} = R_{\text{cy}}$ ,  $K = 0$  and  $2H = 1/R_{\text{cy}} = -h_1^1$ . Especially,  $\Gamma_{ij}^k = 0$ .

#### 5.1 Free cylinder

The simplest example is that of a free cylinder, *i.e.* a cylinder which does not wet a substrate. The contact angle is here  $\theta = \pi$  and thus only normal displacements have to be taken into account, *i.e.*  $\eta^i \equiv 0$  holds. To proceed, denote by  $L$  the length of the cylinder. Then, conservation of volume implies

$$\delta V = \int dA (\psi + H\psi^2) = 0. \quad (48)$$

The second variation of the free energy becomes here

$$\delta^{(2)}F = \int dA \left( \frac{1}{2} \psi^i \psi_i - 2H^2 \psi^2 \right). \quad (49)$$

Due to the symmetries in  $\varphi$  and  $z$  the second variation becomes diagonal for

$$\psi(z, \varphi) = \sum_{m,n} b_{m,n} \psi_{m,n} \equiv \sum_{m,n} b_{m,n} e^{in2\pi z/L} e^{im\varphi}, \quad (50)$$

with  $b_{-m,-n}^* = b_{m,n}$ . The coefficient  $b_{0,0}$  is determined by the conservation of the volume

$$b_{0,0} = -\frac{1}{2R_{\text{cy}}} \sum_{m,n} |b_{m,n}|^2. \quad (51)$$

The function  $\psi_{0,0} \equiv 1$  is an eigenfunction, implying thus  $\int dA \psi_{m,n} = 0$  for  $m \neq 0$  or  $n \neq 0$ . Conservation of volume thus determines only the coefficient  $b_{0,0}$ . Since it is already of second order, this volume reducing mode does not contribute to the second variation. This implies for  $\delta^{(2)}F$

$$\delta^{(2)}F = \frac{\pi L}{R_{\text{cy}}} \sum_{m,n} |b_{m,n}|^2 \left( m^2 + \left( \frac{2\pi R_{\text{cy}}}{L} \right)^2 n^2 - 1 \right). \quad (52)$$

Thus, the free cylinder becomes unstable (for  $m = 0$ ) if  $L/R_{\text{cy}}$  becomes sufficiently large. This is the well-known Plateau-Rayleigh instability, see *e.g.* references [35, 36].

#### 5.2 Cylindrical segment or channel on a homogeneous substrate

Here  $0 < \theta(p) = \theta < \pi$  holds for all  $p \in \partial R$ . Since the stationary state has a translational symmetry no tangential displacements along the  $z$ -axis have to be taken into account, *i.e.*  $\eta^2 \equiv 0$ ,  $\eta^1 = \eta^1(\varphi, z) \neq 0$ . Furthermore,  $C(s) \equiv 0$  holds in this geometry. Equation (35) and the conditions  $X_1(\varphi = 0, z) = -R_{\text{cy}}T(\varphi = 0, z)$  and  $X_1(\varphi = 2\theta, z) = R_{\text{cy}}T(\varphi = 2\theta, z)$  imply

$$\eta^1(0, z) = \frac{1}{R_{\text{cy}}} \xi(0, z) = -\frac{1}{R_{\text{cy}}} \psi(0, z) \cotan \theta \quad (53)$$

$$\eta^1(2\theta, z) = \frac{1}{R_{\text{cy}}} \xi(2\theta, z) = \frac{1}{R_{\text{cy}}} \psi(2\theta, z) \cotan \theta \quad (54)$$

for arbitrary  $z$ . The second variation of the free energy now becomes

$$\delta^{(2)}F = \int dA \left( \frac{1}{2} \psi^i \psi_i - 2H^2 \psi^2 - H\psi \eta_1^1 - H\psi_1 \eta^1 \right). \quad (55)$$

As already mentioned,  $\eta^1$  can be chosen in such a way that it contributes only locally at the contact line. For example,  $\eta^1$  can be defined as a bell function. Then,  $\eta^1$  has the properties (see *e.g.* Ref. [37])

$$\eta^1(\varphi) = C_1 \quad \text{for } 2\theta - \alpha_1 \leq \varphi \leq 2\theta + \alpha_1 \quad (56)$$

$$\eta^1(\varphi) = C_2 \quad \text{for } -\alpha_2 \leq \varphi \leq \alpha_2 \quad (57)$$

$$\eta^1(\varphi) = 0 \quad \text{for } \alpha_2 + \varepsilon_2 \leq \varphi \leq 2\theta - \alpha_1 - \varepsilon_1, \quad (58)$$

see Figure 5. Equations (53, 54) determine the  $\varphi$ -independent functions  $C_1 = C_1(z) \equiv (1/R_{\text{cy}})\psi(2\theta, z)\cotan\theta$  and  $C_2 = C_2(z) \equiv -(1/R_{\text{cy}})\psi(0, z)\cotan\theta$ . Here, the values of  $\varepsilon_i > 0$  and  $\alpha_i > 0$  with  $i = 1, 2$  have to be chosen

appropriately. By using the integral version of the mean-value theorem one obtains

$$\left| \int_{2\theta-\alpha_1-\varepsilon_1}^{2\theta-\alpha_1} d\varphi \psi_1(\varphi) \eta^1(\varphi) \right| = \left| \psi_1(\bar{\varphi}) \int_{2\theta-\alpha_1-\varepsilon_1}^{2\theta-\alpha_1} d\varphi \eta^1(\varphi) \right| < |\psi_1(\bar{\varphi}) C_1^2| \quad (59)$$

with  $2\theta - \alpha_1 - \varepsilon_1 \leq \bar{\varphi} \leq 2\theta - \alpha_1$ . The last inequality holds if one chooses  $\varepsilon_1 \equiv |C_1|$ . Furthermore,

$$\left| \int_{2\theta-\alpha_1}^{2\theta} d\varphi \psi_1 \eta^1 \right| = |\alpha_1 C_1 \psi_1(2\theta)| + \mathcal{O}(\alpha_1^2 C_1). \quad (60)$$

Similar results hold locally at 0. By choosing  $\alpha_i \equiv |C_i|$ , one obtains

$$\int_0^{2\theta} d\varphi \psi_1 \eta^1 = 0 + \mathcal{O}(\psi^3). \quad (61)$$

By performing a partial integration one ends up with

$$\begin{aligned} \int_0^{2\theta} d\varphi \psi \eta_{,1}^1 &= \psi \eta^1 \Big|_0^{2\theta} + \mathcal{O}(\psi^3) \\ &= \frac{1}{R_{\text{cy}}} (\psi^2(2\theta) + \psi^2(0)) \cotan\theta. \end{aligned} \quad (62)$$

Therefore, the second variation of the free energy is given by

$$\begin{aligned} \delta^{(2)} F &= R_{\text{cy}} \int_0^L dz \int_0^{2\theta} d\varphi \left\{ \frac{1}{2} \psi^i \psi_i - 2H^2 \psi^2 \right. \\ &\quad \left. - \frac{H}{R_{\text{cy}}} \psi^2 \cotan\theta (\delta(\varphi - 2\theta) + \delta(\varphi)) \right\}. \end{aligned} \quad (63)$$

The translational symmetry in the  $z$ -direction suggests the ansatz

$$\psi(\varphi, z) = \sum_n b_n e^{in2\pi z/L} f(\varphi). \quad (64)$$

By performing a partial integration one obtains

$$\delta^{(2)} F = \frac{L}{2R_{\text{cy}}} \sum_n |b_n|^2 \int_0^{2\theta} d\varphi f(\varphi) \widehat{D} f(\varphi), \quad (65)$$

with the differential operator

$$\begin{aligned} \widehat{D} &\equiv -\frac{d^2}{d\varphi^2} + (\delta(\varphi - 2\theta) - \delta(\varphi)) \frac{d}{d\varphi} + \left( \frac{2\pi R_{\text{cy}}}{L} n \right)^2 \\ &\quad - 1 - \cotan\theta (\delta(\varphi - 2\theta) + \delta(\varphi)). \end{aligned} \quad (66)$$

Diagonalizing the operator of the second variation is equivalent to finding a solution of the differential equation

$$\widehat{D} f = \lambda_n(\theta) f, \quad \lambda_n(\theta) = \left( \frac{2\pi R_{\text{cy}}}{L} n \right)^2 n^2 - 1 - \lambda(\theta). \quad (67)$$

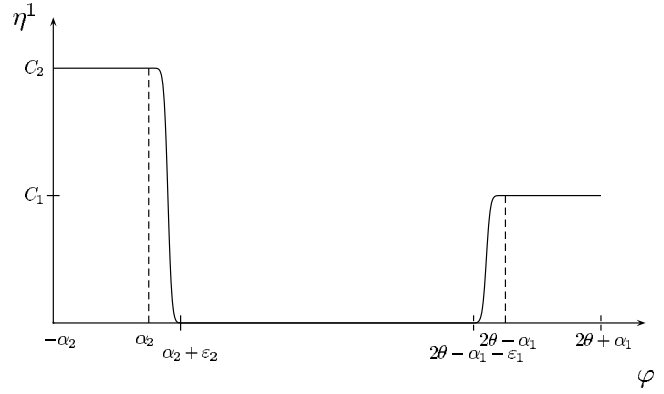


**Fig. 5.** Definition of  $\eta^1$  as a bell function.  $\eta^1$  has thus constant values  $C_1$  and  $C_2$  for  $2\theta - \alpha_1 \leq \varphi \leq 2\theta + \alpha_1$  and  $-\alpha_2 \leq \varphi \leq \alpha_2$ , respectively. The regions in which  $\eta^1$  drops to 0 have widths  $\varepsilon_1$  and  $\varepsilon_2$ .

Here,  $\lambda(\theta)$  denotes the shift of the eigenvalues caused by  $f(\varphi)$ , see equation (52). In Appendix C the solution of this differential equation is derived.

By using the explicit solution (C.4) and equation (C.3) one can show that the eigenvalues are determined by

$$\tan\left(2\theta\sqrt{-\lambda(\theta)}\right) = \frac{2\sqrt{-\lambda(\theta)}\cotan\theta}{\cotan^2\theta + \lambda(\theta)}. \quad (68)$$

This equation reads for  $\lambda > 0$

$$\tanh\left(2\theta\sqrt{\lambda(\theta)}\right) = \frac{2\sqrt{\lambda(\theta)}\cotan\theta}{\cotan^2\theta + \lambda(\theta)}. \quad (69)$$

In the following, one can restrict the discussion to the positive branches  $\sqrt{\lambda} > 0$  and  $\sqrt{-\lambda} > 0$ . The left hand side of equation (68) is positive for  $\lambda > 0$ , whereas it can be positive or negative for  $\lambda < 0$ . For  $\lambda > 0$  the right hand side is positive only for  $\theta < \pi/2$ . Thus, the eigenvalues can only be positive for  $\theta < \pi/2$ . The right hand side of equation (68) goes to 0 for large  $\lambda$ , the left hand side goes to 1. In this case, there is exactly one positive eigenvalue. For small  $\theta$  the left hand side of equation (69) goes to 1. In this case,  $\lambda(\theta) \approx 1/\theta^2$  holds in agreement with reference [20]<sup>5</sup>.

For  $\theta > \pi/2$  only negative eigenvalues  $\lambda < 0$  exist. Here, only the eigenvalues of minimal absolute value are of interest. Then,  $\lambda(\theta)$  is monotonously decreasing in  $\theta$ , with  $\lambda(\pi) = -1/4$ , see Figure 6.

One should note, that the cases  $\theta = \pi/2$  and  $\theta = \pi$  are special. For  $\theta = \pi/2$  the eigenvalues are determined by  $\tan(\sqrt{-\lambda}2\theta) = 0$ , *i.e.*  $\lambda = -m^2$ , with  $m = 1, 2, \dots$ , in agreement with Section 5.1. For  $\theta = \pi$  in equation (C.4)  $f(0) = f(2\pi)$  must hold, *i.e.*  $\lambda = -m^2$ . Generally, for large  $|\lambda|$  the spectrum becomes discrete,  $\lambda \sim -(m\pi/2\theta)^2$ , with a constant correction to the free cylinder.

The fact, that for all  $\theta$  an eigenvalue  $\lambda(\theta) > -1$  exists implies that the cylindrical segments become

<sup>5</sup> In reference [20] the stability of cylindrical segments on homogeneous substrates has been investigated in the limit of small contact angles  $\theta \ll 1$ .

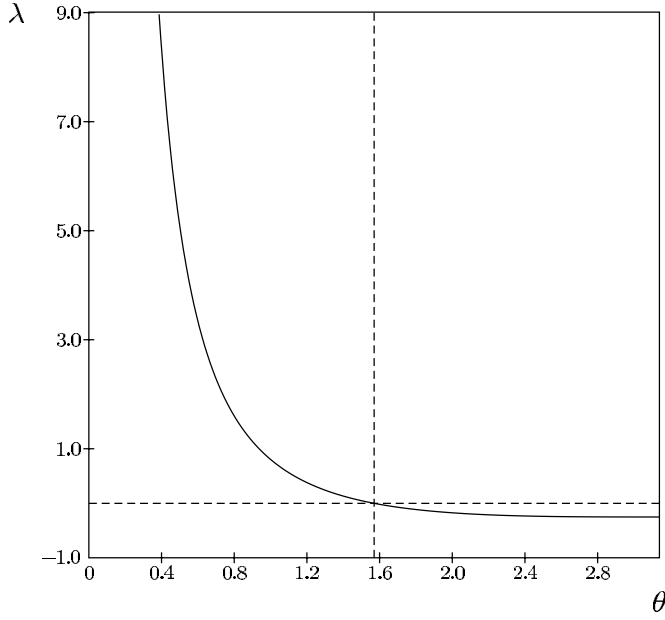


**Fig. 6.** Largest eigenvalue  $\lambda$  as function of the contact angle  $\theta$  as obtained from the second variation of the free energy of a cylindrical segment on a homogeneous substrate, see equation (68).

unstable, as can be seen by considering *e.g.*  $\psi(\varphi, z) = f_\lambda(\varphi)[b_0 + b_1 e^{i2\pi z/L}]$ . Then, conservation of volume again only determines the coefficient  $b_0$  (which is of second order). Therefore, the second variation of the free energy  $\delta^{(2)}F$  becomes negative for sufficiently large  $L/R_{cy}$ . Hence, cylindrical segments of arbitrary contact angles on homogeneous substrates are unstable. This instability has been experimentally observed for instance in [38].

### 5.3 Channel on a hydrophilic stripe

Here, a cylindrical segment wetting a hydrophilic stripe ( $\gamma$ ) shall be examined, which belongs to droplet regime (II). Hence,  $\theta_\gamma < \theta < \theta_\delta$ . In order to determine the stability of this droplet one has to distinguish between those variations of the shape which displace the contact line and those which leave it fixed.

#### (i) Variations with displaced contact line

Here, one has to take into account the transition region between ( $\gamma$ ) and ( $\delta$ ). As shown in reference [13] it is useful to consider first a transition region which has finite width. For stripes one can introduce local coordinates  $x$  and  $z$ , where the line  $x = 0$  lies in the middle of the domain. Thus, generally  $\theta$  will depend on  $x$  and  $z$ . If only transition regions are considered which are translational invariant in the  $z$ -direction and symmetric with respect to  $x = 0$ , then  $\theta(x) = \theta_\gamma$  holds for  $|x| \leq (a_\gamma - a)/2$  and  $\theta(x) = \theta_\delta$  holds for  $|x| > (a_\gamma + a)/2$ . Here,  $a_\gamma$  is the width of the stripe,  $a$  the width of the transition region and  $x = x(z)$  the

position of the contact line. Then, one obtains for  $x > 0$  the first order contribution

$$\begin{aligned} \delta^{(1)}F_{\beta w} &= 2 \int_0^L dz \tan(\theta(x))\psi \\ &= 2 \int_0^L dz \tau(z) \cos(\theta(x)). \end{aligned} \quad (70)$$

Together with equation (42) this yields the generalized Young equation  $\cos \theta = \cos \theta(x)$ , in accordance with reference [13]. The second order contribution is given by

$$\delta^{(2)}F_{\beta w} = - \int_0^L dz \psi^2(z) \frac{d\theta(x)/dx}{\sin \theta(x)}. \quad (71)$$

Here, the derivative  $d\theta(x)/dx$  is of the order  $1/a$ . As the width of transition region tends to zero,  $a \rightarrow 0$ , this term becomes dominant in the second variation of the free energy, since the linear stability analysis is only valid, if  $|\psi| \ll a$  holds locally at the domain border. Equations (53, 54) then imply  $|\eta^1| \ll a$ . If  $\theta_\gamma < \theta_\delta$  then  $d\theta(x)/dx$  is positive and for small width  $a$  the remaining contributions to  $\delta^{(2)}F$  are negligible. Hence,  $\delta^{(2)}F > 0$  for  $\theta_\gamma < \theta < \theta_\delta$  and for variations which displace the contact line. For  $a \rightarrow 0$  also  $\psi|_{\partial X} \rightarrow 0$  must hold. In the limit of a sharp transition region only variations are allowed which keep the contact line fixed since in this limit the generalized forces  $\delta F/\delta x$  associated with an displacement  $\delta x$  of the contact line diverge. For  $\theta = \theta_\delta$  this argumentation does no longer hold, since these channels can be unstable against variations of their shape which displace the contact line, as seen in the last section.

Thus, the structure of the substrate stabilizes cylindrical segments belonging to droplet regime (II) against variations of their shape which displace the contact line. However, these channels can be unstable against variations which keep the contact line fixed, as will be shown now.

#### (ii) Variations with fixed contact line

Here, the variations fulfil the special boundary condition

$$\psi(0, z) = \psi(2\theta, z) = 0. \quad (72)$$

Hence, only normal displacements have to be considered, *i.e.*  $\eta^i \equiv 0$ . The symmetry of the problem suggests the ansatz

$$\psi(\varphi, z) = \sum_{m,n} b_{m,n} e^{in2\pi z/L} \sin(m\pi\varphi/2\theta), \quad (73)$$

with  $m = 1, 2, \dots$  and  $b_{m,n} = b_{m,-n}^*$ . Conservation of volume yields the quadratic equation for  $b_{m',0}$ , with  $m' = 1, 3, 5, \dots$

$$\begin{aligned} \sum_{m=1,3,5,\dots} \left( \frac{b_{m,0}}{m} + \frac{\pi}{8R_{cy}} \sum_n |b_{m,n}|^2 \right) = \\ - \frac{\pi}{8R_{cy}} \sum_{m=2,4,6,\dots} \sum_n |b_{m,n}|^2, \end{aligned} \quad (74)$$

which has the solution

$$b_{m,0} = -m \frac{\pi}{8R_{cy}} \sum_{n \neq 0} (|b_{m+1,n}|^2 + |b_{m,n}|^2) + \mathcal{O}(|b_{m,n}|^4). \quad (75)$$

The second variation of the free energy is given by

$$\delta^{(2)}F = \frac{L\theta}{2R_{cy}} \sum_{m,n} |b_{m,n}|^2 \left( \frac{m^2\pi^2}{4\theta^2} + \left( \frac{2\pi R_{cy}}{L} \right)^2 n^2 - 1 \right). \quad (76)$$

Hence, the cylindrical segment is stable against disturbances with  $m \geq 2$ . For  $m = 1$  the channel becomes unstable, *i.e.*  $\delta^{(2)}F \leq 0$  if

$$L^2 \left( 1 - \frac{m^2\pi^2}{4\theta^2} \right) \geq (2\pi R_{cy})^2. \quad (77)$$

Thus, cylindrical segments on stripe domains with contact angle  $\theta > \pi/2$  are unstable against variations which rearrange the liquid within the droplet by keeping the contact line fixed. This novel instability has indeed been observed experimentally, see reference [12].

#### 5.4 Other surface domain geometries

The general stability criterion can now be applied to other surface domains and droplet morphologies. As an example, it is possible to show that spherical droplets are stable for arbitrary contact angle  $\theta$ . This holds both for homogeneous substrates and for droplets belonging to regime (II) on structured substrates with circular domains. Furthermore, it is possible to show rigorously that for arbitrary surface domain geometries the droplets of regime (II), *i.e.* the droplets covering the domain completely, are stabilized against variations of their shape which displace the contact line if  $\theta(s) < \theta_\delta$  holds everywhere. This result can be obtained by generalizing the argument involving the separation of length scales of the last section to arbitrary domain geometries. However, the corresponding calculations are straightforward and shall not be given here.

## 6 Summary and outlook

In summary, we have studied the stability of various wetting morphologies on homogeneous and structured surfaces. On the latter substrates, the free energy of the droplet depends on the geometry of the system, *i.e.* it depends on the underlying structure of the substrate. As shown, the local calculus of differential geometry provides the appropriate framework to treat this functional dependence analytically. Using this approach, it is possible to rigorously derive the conditions for the stationary states, *i.e.* the Laplace equation and the generalized Young equation. By performing the second variation of the free energy, a coordinate independent stability criterion is obtained

which is valid for arbitrary droplet morphologies on arbitrary surface domains. The application of this criterion to liquid channels shows that these morphologies of the wetting layer are unstable on homogeneous substrates against shape deformations which displace the contact line. On appropriately structured surfaces, these channels are stabilized against such perturbations, but can exhibit a new kind of instability characterized by a rearrangement of the liquid within the droplet at fixed contact line. This difference between the instabilities of droplets on homogeneous and appropriately structured substrates is fundamental. Droplets of regime (II), *i.e.* droplets covering a domain completely, are generally stabilized by the substrate-structure against displacements of their contact line.

The theoretical approach used here can be extended in various ways. For example, one may consider different wetting geometries such as ring-shaped surface domains or the interaction of two structured surfaces arising from stabilized liquid bridges.

The ambition of the experimental groups working in this field is to create smaller and smaller surface patterns with domain sizes in the nanometer range. For sufficiently small structures, the morphology will no longer be governed by the interfacial tensions alone but will also depend on the contact line tension. As discussed in reference [10], these line tension contributions should become noticeable as soon as the linear dimension  $L_\beta$  of the wetting structures is a few hundreds nanometers, and they should become rather strong for  $L_\beta \simeq 30$  nm.

From a theoretical point of view, the line tension makes additional contributions to the generalized Young equation as recently derived for location-dependent line tensions [30]. The corresponding free energy term will also change the stability of the wetting morphologies but a general stability analysis which includes line tension terms remains to be done [39].

We thank W. Fenzl, G. Gompper, S. Herminghaus, P. Leiderer, U. Seifert and P. Swain for valuable discussions.

## Appendix A: The Levi-Civita symbol

In this appendix a collection of useful formulas related to the Levi-Civita symbol is given.

The Levi-Civita symbol in 2 dimensions is defined as [40]

$$\varepsilon^{ij} \equiv \delta_1^i \delta_2^j - \delta_2^i \delta_1^j, \quad \varepsilon_{ij} \equiv \varepsilon^{ij}, \quad (A.1)$$

where  $\delta_i^j$  denotes the Kronecker delta, *i.e.*  $\delta_i^j = 0$  for  $j \neq i$  and  $\delta_i^i = 1$  for  $i = j$ .

As can be easily seen, one has the general relation

$$\varepsilon_{ij} \varepsilon^{mn} = \delta_i^m \delta_j^n - \delta_j^m \delta_i^n. \quad (A.2)$$

This implies for an arbitrary second-rank tensor  $A \equiv ((a_{ij}))$

$$\det(A) \varepsilon_{ij} = \varepsilon^{kl} a_{ik} a_{jl}. \quad (A.3)$$

Contracting this expression with  $\varepsilon^{ij}$ , the determinant of  $A$  can thus be written as

$$\det(A) = \frac{1}{2}\varepsilon^{ij}\varepsilon^{kl}a_{ik}a_{jl}. \quad (\text{A.4})$$

In particular, one obtains then for the first fundamental form

$$g \equiv \det(g_{ij}) = \frac{1}{2}\varepsilon^{ij}\varepsilon^{kl}g_{ik}g_{jl}. \quad (\text{A.5})$$

The inverse of  $A$  is given by

$$(A^{-1})^{ij} = \frac{1}{\det(A)}\varepsilon^{ik}\varepsilon^{jl}a_{lk}. \quad (\text{A.6})$$

This implies correspondingly for the first fundamental form  $G \equiv (g_{ij})$

$$g^{ij} \equiv (G^{-1})^{ij} = \frac{1}{g}\varepsilon^{ik}\varepsilon^{jl}g_{kl}. \quad (\text{A.7})$$

To proceed, denote by  $a_i^j, b_i^j$  arbitrary second-rank tensors. Then, the tensor indices can be raised and lowered *via* the first fundamental form

$$a_{ij}g^{jk} = a_i^k, \quad a_i^k g_{kj} = a_{ij}, \quad \text{etc.} \quad (\text{A.8})$$

By using equation (A.3) the following identity can be shown

$$\varepsilon^{ik}\varepsilon^{jl}a_{ij}b_{kl} = g\varepsilon^{ik}\varepsilon_{jl}a_i^j b_k^l. \quad (\text{A.9})$$

This implies especially,

$$\det(a_i^j) = \frac{\det(a_{ij})}{g}. \quad (\text{A.10})$$

Finally, one should note that  $\varepsilon^{ij}$  does not transform as a tensor. To obtain the completely antisymmetric tensor one has to define

$$\tilde{\varepsilon}_{ij} \equiv g\varepsilon^{ij}. \quad (\text{A.11})$$

In this case  $\tilde{\varepsilon}_{kl} = \tilde{\varepsilon}^{ij}g_{ik}g_{jl}$  holds.

## Appendix B: Change of volume

Here, it is shown that the side faces do not contribute in second order to the change of volume  $\delta V$  caused by the displacement  $R' - R$ . By using the notation of Section 4.3 and defining  $v \equiv \psi N + \eta^i R_i$  one can enumerate the side faces from 1 to 4 in a counterclockwise fashion, starting with the side face spanned by  $R_1 ds^1$  and  $v$ . Then, up to order  $\mathcal{O}(\psi, \eta)$  the normal  $\nu^{(i)}$  of the side face (i) is given by

$$\nu^{(1)} = (R_1 ds^1) \times v \quad (\text{B.1})$$

$$\nu^{(2)} = (R_2 ds^2) \times (v + (R'_1 - R_1) ds^1) \quad (\text{B.2})$$

$$\nu^{(3)} = (v + (R'_1 - R_1) ds^1 + (R'_2 - R_2) ds^2) \times (R_1 ds^1) \quad (\text{B.3})$$

$$\nu^{(4)} = v \times (R_2 ds^2), \quad (\text{B.4})$$

since  $R'_i$  and  $R_i$  differ only by  $\mathcal{O}(\psi, \eta)$ . The vector  $m^{(i)}$  pointing from the origin to the center of mass of face (i) is given by

$$m^{(1)} = \frac{1}{4}(R_1 + R'_1) ds^1 \quad (\text{B.5})$$

$$m^{(2)} = \frac{1}{2}(R_1 + R'_1) ds^1 + \frac{1}{4}(R_2 + R'_2) ds^2 \quad (\text{B.6})$$

$$m^{(3)} = \frac{1}{4}(R_1 + R'_1) ds^1 + \frac{1}{2}(R_2 + R'_2) ds^2 \quad (\text{B.7})$$

$$m^{(4)} = \frac{1}{4}(R_2 + R'_2) ds^2. \quad (\text{B.8})$$

Thus, for the side face (i)

$$\begin{aligned} z e_z dA &= m^{(i)} \cdot \frac{v}{|v|} \left( \frac{v}{|v|} \cdot \nu^{(i)} \right) \\ &= 0 + \mathcal{O}((ds^1)^2 ds^2, ds^1 (ds^2)^2). \end{aligned} \quad (\text{B.9})$$

The last identity holds since  $|m^{(i)}|$  is of order  $\mathcal{O}(ds^1, ds^2)$  and the deviation of  $v \cdot \nu^{(i)}$  from 0 is at least of order  $\mathcal{O}((ds^1)^2, ds^1 ds^2, (ds^2)^2)$ . Hence, the side faces do not contribute to  $\Delta V$  as given by (38).

## Appendix C: Channel eigenmodes for homogeneous substrate

Here, the solution to the differential equation (67) is derived by performing a Laplace-transformation. Then, the differential equation becomes an algebraic equation in  $Y(s) \equiv \int_0^\infty d\varphi f(\varphi) e^{-s\varphi}$

$$\begin{aligned} Y(s) &= \frac{1}{s^2 - \lambda(\theta)} (f(0)(s - \cotan\theta) \\ &\quad - \cotan\theta f(2\theta) e^{-2s\theta} + f'(2\theta) e^{-2s\theta}), \end{aligned} \quad (\text{C.1})$$

with  $f'(\varphi) \equiv df/d\varphi$ . By transforming back, one obtains the function  $\tilde{f}(\varphi)$

$$\begin{aligned} \tilde{f}(\varphi) &= f(0) \cos\left(\sqrt{-\lambda(\theta)}\varphi\right) \\ &\quad - \frac{f(0)\cotan\theta}{\sqrt{-\lambda(\theta)}} \sin\left(\sqrt{-\lambda(\theta)}\varphi\right) \\ &\quad + \frac{\sin\left(\sqrt{-\lambda(\theta)}(\varphi - 2\theta)\right)}{\sqrt{-\lambda(\theta)}} (f'(2\theta) - f(2\theta)\cotan\theta). \end{aligned} \quad (\text{C.2})$$

The function  $\tilde{f}(\varphi)$  is a solution  $f(\varphi)$  of the differential equation if it fulfills the self-consistency condition  $\tilde{f}(0) = f(0)$ . Hence

$$f'(2\theta) - f(2\theta)\cotan\theta = 0. \quad (\text{C.3})$$

The eigenfunctions to the eigenvalue  $\lambda(\theta)$  are then given by

$$\begin{aligned} f_\lambda(\varphi) &= f(0) \left\{ \cos\left(\sqrt{-\lambda(\theta)}\varphi\right) \right. \\ &\quad \left. - \sin\left(\sqrt{-\lambda(\theta)}\varphi\right) \frac{\cotan\theta}{\sqrt{-\lambda(\theta)}} \right\}. \end{aligned} \quad (\text{C.4})$$

One should note that the solution is not symmetric in  $\varphi$ . The eigenvalues  $\lambda(\theta)$  are determined by equations (68, 69) as can be seen by using equations (C.4, C.3).

Finally, the meaning of the self-consistency condition becomes clear if equation (C.4) is used as an ansatz for the solution. Then, equation (C.4) is a solution of the differential equation if and only if equation (C.3) is fulfilled. Equation (68) guarantees the orthogonality of the eigenfunctions  $f_{\lambda_1}$  and  $f_{\lambda_2}$  to different eigenvalues  $\lambda_1 \neq \lambda_2$  on the interval  $[0, 2\theta]$ .

## Appendix D: List of symbols

$A_{ij}$	surface area of interfacial region between phase ( $i$ ) and phase ( $j$ ),
$C(s)$	curvature of the contact line,
$\widehat{C}_i, \alpha_i, \varepsilon_i$	constants characterizing bell function,
$\widehat{D}$	differential operator,
$dA = dA_{\alpha\beta}$	surface area element of the ( $\alpha\beta$ ) interface of the droplet,
$dA_{\beta w}$	area element of the contact area of the droplet
$dV$	volume element,
$\delta^{(1)}F_{1d}$	terms of first variation contributing to the generalized Young equation,
$\delta^{(1)}F_{2d}$	terms of first variation contributing to the Laplace equation,
$\delta^{(1)}F_{\alpha\beta}^*$	contribution from $\delta^{(1)}F_{\alpha\beta}$ to $\delta^{(1)}F_{1d}$ ,
$\delta^{(2)}F$	second variation of $F$ ,
$\partial R(s) \equiv R _{\partial\Omega}$	contact line parameterized by arclength $s$ ,
$\varepsilon^{ij}$	Levi-Civita symbol,
$\eta^i$	coefficients of the tangential component of $R' - R$ ,
$\theta_{\beta w}$	contact angle defined by equation (2),
$\theta_\gamma$	contact angle on ( $\gamma$ ),
$\theta_\delta$	contact angle on ( $\delta$ ),
$\theta(s)$	local contact angle of the droplet
$F$	free energy,
$F_{\alpha\beta}$	( $\alpha\beta$ ) interfacial free energy,
$F_{\beta w}$	interfacial free energy of contact area,
$f, \tilde{f}$	solutions to differential equation,
$g_{ij}$	first fundamental form,
$g$	determinant of first fundamental form,
$\Gamma_{ij}^k$	Christoffel symbols,
$H$	mean curvature,
$h_{ij}$	second fundamental form,
$K$	Gaussian curvature,
$L$	length of cylinder,
$\lambda$	shift of $\lambda_n$ due to $f$ ,
$\lambda_n$	eigenvalue,
$N$	(surface) normal vector,
$n(s)$	normal vector of $\partial R(s)$ ,
$\xi(s)$	arbitrary function at the contact line,
$\xi_i^k, \nu_i, A_{ij}$ ,	
$\delta g_1, \lambda_{kl}$	abbreviations,
$\Delta P$	pressure difference between ( $\alpha$ ) and ( $\beta$ ),
$R(s^1, s^2)$	surface vector,
$R_{cy}$	radius of cylinder,

$R_i$	(surface) tangent vector,
$s^i$	local coordinates,
$\Sigma_{ij}$	interfacial tension between phase ( $i$ ) and phase ( $j$ ),
$T(s)$	tangent vector of $R(\omega(s))$ ,
$t(s)$	tangent vector of $\partial R(s)$ ,
$\tau(s)$	arbitrary function at the contact line,
$Y(s)$	Laplace transform of $f$ ,
$\psi$	coefficient of the normal component of $R' - R$ ,
$\Omega$	parameter domain of $R(s^1, s^2)$ ,
$\omega(s)$	representation of $\partial\Omega$ .

## References

1. K. Jacobs, H. Gau, S. Schlagowski, W. Mönch, T. Pompe, A. Fery, S. Herminghaus, in *Proc. 2nd European Coating Symp.*, Strasbourg, 1997.
2. F. Burmeister, C. Schäfle, T. Matthes, M. Böhmisch, J. Boneberg, P. Leiderer, *Langmuir* **13**, 2983 (1997).
3. J. Heier, E.J. Kramer, S. Waldheim, G. Krausch, *Macromolecules* **30**, 6610 (1997).
4. G.P. Lopez, H.A. Biebuyck, C.D. Frisbie, G.M. Whitesides, *Science* **260**, 647 (1993).
5. J. Drelich, J.D. Miller, A. Kumar, G.M. Whitesides, *Coll. Surf. A* **93**, 1 (1994).
6. F. Morhard, J. Schumacher, A. Lenebach, T. Wilhelm, R. Dahint, M. Grunze, D.S. Everhart, *Electrochem. Soc. Proc.* **97**, 1058 (1997).
7. G. Möller, M. Harke, H. Motschmann, D. Prescher, *Langmuir* **14**, 4955 (1998).
8. R. Wang, K. Hashimoto, A. Fujishima, *Nature* **388**, 431 (1997).
9. U. Drodofsky, J. Stuhler, T. Schulze, M. Drewsen, B. Brezger, T. Pfau, J. Mlynek, *Appl. Phys. B* **65**, 755 (1997).
10. R. Lipowsky, P. Lenz, P.S. Swain, *Coll. Surf. A* **161**, 3 (2000).
11. P. Lenz, *Adv. Mater.* **11**, 1531 (1999).
12. H. Gau, S. Herminghaus, P. Lenz, R. Lipowsky, *Science* **283**, 46 (1999).
13. P. Lenz, R. Lipowsky, *Phys. Rev. Lett.* **80**, 1920 (1998).
14. C. Bauer, S. Dietrich, A.O. Parry, *Europhys. Lett.* **47**, 474 (1999).
15. E. Raphael, *C.R. Acad. Sci. Paris* **306**, 751 (1988).
16. T. Odarcuhu, *J. Phys. II France* **5**, 227 (1995).
17. M. Struwe, *Plateau's problem and the calculus of variations* (Princeton Univ. Press, NJ, 1988).
18. J. Sullivan, F. Morgan, *Int. J. Math.* **7**, 833 (1996).
19. P. Lenz, R. Lipowsky (in preparation).
20. K. Sekimoto, R. Oguma, K. Kawasaki, *Ann. Phys.* **176**, 359 (1987).
21. U. Seifert, *Phys. Rev. A* **43**, 6803 (1991).
22. U. Dierkes, S. Hildebrandt, A. Küster, O. Wohlrab, *Minimal Surfaces I* (Springer, Berlin, 1992).
23. Ou-Yang Zhong-can, W. Helfrich, *Phys. Rev. A* **39**, 5280 (1989).
24. S. Komura, R. Lipowsky, *J. Phys. II France* **2**, 1563 (1992).
25. R. Finn, *Equilibrium capillary surfaces* (Springer, New York, 1986).
26. G.I. Taylor, D.H. Michael, *J. Fluid Mech.* **58**, 625 (1973).

27. A. Sharma, E. Ruckenstein, *J. Coll. Interf. Sci.* **133**, 358 (1989).
28. F. Brochard-Wyart, J. Daillant, *Can. J. Phys.* **68**, 1084 (1990).
29. B. Widom, *J. Phys. Chem.* **99**, 2803 (1995).
30. P.S. Swain, R. Lipowsky, *Langmuir* **14**, 6772 (1998).
31. See, *e.g.*, R. Lipowsky, *Phys. Rev. Lett.* **52**, 1429 (1984); R. Lipowsky, M.E. Fisher, *Phys. Rev. B* **36**, 2126 (1987).
32. W. Koch, S. Dietrich, M. Napiorkowski, *Phys. Rev. E* **51**, 3300 (1995).
33. P.R. Halmos, *Finite-dimensional vector spaces* (van Nostrand Reinhold Company, New York, 1958).
34. E. Kreyszig, *Differential geometry* (Dover, New York, 1991).
35. S. Chandrasekhar, *Hydrodynamic and hydromagnetic stability* (Dover, New York, 1981).
36. T.E. Faber, *Fluid dynamics for physicists* (Cambridge Press, Cambridge, 1995).
37. Th. Bröcker, *Analysis I* (B.I., Mannheim, 1992).
38. T. Ondarcuhu, M. Veyssie, *Nature* **352**, 418 (1991).
39. P. Lenz, in preparation.
40. B.F. Schutz, *Geometrical methods in mathematical physics* (Cambridge Univ. Press, Cambridge, 1980).